

Synthesis and Crystal Structure of Mn_4As_3 and Its Relation to Other Manganese Arsenides

Martin F. Hagedorn and Wolfgang Jeitschko

Anorganisch-Chemisches Institut, Universität Münster, Wilhelm-Klemm-Strasse 8, D-48149 Münster, Germany

Received February 6, 1995; in revised form May 31, 1995; accepted June 8, 1995

The title compound was prepared by reaction of the elements at 700°C in the presence of iodine. Its crystal structure—determined from single-crystal diffractometer data—is isotypic with that of $\beta\text{-V}_4\text{As}_3$: $C2/m$, $a = 1341.1(2)$ pm, $b = 369.34(5)$ pm, $c = 962.8(1)$ pm, $\beta = 101.97(1)^\circ$, and $R = 0.027$ for 1394 structure factors and 62 variable parameters. Mn_4As_3 is the member with $n = 2$ of a series of closely related structures with the general composition $\text{Mn}_{2+n}\text{As}_{1+n}$. Other members of this series are the modification III of Mn_3As_2 (with $n = 1$) and the two closely related structures of MnAs (with $n = \infty$). The structural relationships of these compounds and the other known manganese arsenides Mn_2As , $\text{Mn}_3\text{As}_2(\text{I})$, $\text{Mn}_3\text{As}_2(\text{II})$, and Mn_5As_4 are pointed out, emphasizing the numerous Mn–Mn bonds in these arsenides with high manganese content. © 1995

Academic Press, Inc.

INTRODUCTION

In contrast to the binary system manganese–phosphorus which contains three modifications of MnP_4 (1–5), there are no manganese arsenides with a high content of arsenic. Mn_3As (6), two modifications of Mn_2As (7–9), and two modifications of MnAs (10–12) have been known for some time. In addition to these, the phase diagram of the binary system manganese arsenic as reassessed by Okamoto (13) contains several compounds with intermediate compositions. We have already reported Mn_5As_4 (14) and about three modifications of Mn_3As_2 (14–16). According to our investigations only one compound remained with an unknown structure and this is the compound Mn_4As_3 reported here. Its powder pattern shows little resemblance to that of the compound Mn_4As_3 reported by Brauer (17). A preliminary account of our work on Mn_4As_3 was given at a conference (18).

PREPARATION OF MANGANESE ARSENIDES WITHIN THE COMPOSITIONAL RANGE BETWEEN Mn_2As AND MnAs

Originally we attempted to establish the phase diagram of the binary system manganese arsenic. However, because

of contradictions with previously reported experimental results and because of the persistent coexistence of $\text{Mn}_3\text{As}_2(\text{I})$, $\text{Mn}_3\text{As}_2(\text{II})$, and Mn_5As_4 we were not successful in that respect. Nevertheless, we have reproducibly prepared the three modifications of Mn_3As_2 as well as Mn_4As_3 and Mn_5As_4 and their preparation conditions are reported here.

Starting materials were powders of manganese (Heraeus: –325 mesh, 99.5%) and arsenic (Ventron: pieces with diameters of about 1 cm). The arsenic was purified twice by fractional sublimation prior to the reactions. The mixed powders, with starting compositions varying between the atomic ratios Mn:As = 2:1 and 1:1, were annealed in evacuated sealed silica tubes for up to 1 week at temperatures of 600 or 650°C. Frequently the prereacted products were ground to fine powders, pressed to pellets, and annealed again in silica tubes at the desired temperatures. Usually the silica tubes were visibly attacked by the samples, however, the energy dispersive X-ray analyses of the crystals used for the crystal structure determinations did not reveal any silicon. Nevertheless, single-phase products were usually obtained from samples with a slight excess of manganese in the starting composition.

Mn_4As_3 was repeatedly obtained by reacting the powders of the elements for 1 day at 650°C, followed by an annealing of the cold-pressed pellets for 1 day at 700°C. Samples of Mn_4As_3 annealed at 800°C resulted in $\text{Mn}_3\text{As}_2(\text{I})$ and MnAs . The crystals used for the structure analysis were obtained by annealing the prereacted powder in the presence of iodine. Mn_4As_3 can also be prepared from samples of $\text{Mn}_3\text{As}_2(\text{I})$ by heating these samples at temperatures between 580 and 700°C for a few minutes. Crystals of this compound have the form of needles. They are grey with metallic luster.

The low-temperature phase $\text{Mn}_3\text{As}_2(\text{III})$ is obtained by annealing pellets of the prereacted samples for 2 days at temperatures of 650°C or as high as 850°C. Annealing at higher temperatures resulted in $\text{Mn}_3\text{As}_2(\text{I})$. Single crystals of $\text{Mn}_3\text{As}_2(\text{III})$ were obtained by chemical transport as described earlier (16).

The high-temperature phase $\text{Mn}_3\text{As}_2(\text{I})$ can be prepared

TABLE 1
Cell Parameters of Manganese Arsenides in the Range between Mn₂As and MnAs

Compound	Space group	<i>a</i> (pm)	<i>b</i> (pm)	<i>c</i> (pm)	β (°)	<i>V</i> (nm ³)	Ref.
Mn ₃ As ₂ (I)	<i>C2/m</i>	1385.6(6)	377.7(2)	1362.2(8)	107.79(3)	0.6788	(15)
Mn ₃ As ₂ (II)	<i>Cmc2₁</i>	376.1(1)	1376.0(2)	1319.0(1)	90.0	0.6826	(14)
Mn ₃ As ₂ (III)	<i>C2/m</i>	1324.7(3)	369.5(1)	904.6(4)	132.23(3)	0.3279	(16)
Mn ₄ As ₃	<i>C2/m</i>	1341.1(2)	369.34(5)	962.8(1)	101.97(1)	0.4665	this work
Mn ₅ As ₄	<i>Cmc2₁</i>	376.1(1)	1376.0(2)	1212.3(2)	90.0	0.6274	(14)

by a heat treatment of the prereacted samples for 1 day or 1 week at 900°C. Well developed crystals were obtained by longer annealing times. This compound is best retained by quenching the silica tubes in ice water. In contrast to Mn₃As₂(II) and Mn₃As₂(III), the high-temperature phase Mn₃As₂(I) does not have the ideal composition. The structure determination of a single-crystal resulted in the composition Mn_{2.896(1)}As₂ (15) and from the refinements of this structure from data collected of a twinned specimen the compositions Mn_{2.883(3)}As₂ and Mn_{2.89(2)}As₂ were obtained (15). Samples of this high-temperature structure are stable at temperatures as low as 725°C. However, when such samples are kept at 700 or 580°C they decompose within a few minutes to Mn₃As₂(III) and Mn₄As₃.

Both Mn₃As₂(II) and Mn₅As₄ were obtained reproducibly only together as well developed intergrown crystals with dimensions of up to 0.5 × 0.5 × 1 mm³. They are stable at temperatures of 800 and 900°C and are usually attached to the surface of pellets of the high-temperature phase Mn₃As₂(I). As was pointed out above, the exact composition of this phase is Mn_{2.89}As₂. The off-stoichiometry is caused by the partial occupancy of one manganese position, which is tetrahedrally coordinated by arsenic atoms. The closely related structures of the intergrown crystals Mn₃As₂(II) and Mn₅As₄ are both stoichiometric and both have a tetrahedral site coordinated by arsenic atoms. In Mn₃As₂(II) (Mn₆As₄) this site is occupied by manganese atoms and in Mn₅As₄ this site is entirely unoccupied (14). It seems possible that Mn₃As₂(I) (= Mn_{2.89}As₂) is metastable. It may be the first reaction product in this compositional range, which slowly decomposes to the large intergrown crystals of Mn₃As₂(II) and Mn₅As₄ on prolonged heating.

These five phases (Table 1) are the only ones observed by us in the more than 100 samples prepared in the range between Mn₂As and MnAs at various temperatures between 650 and 900°C. The phase diagram as reported by Yuzuri and Yamada (19) and reassessed by Okamoto (13) contains the phases β -Mn₃As₂, α -Mn₃As₂, and Mn₄As₃, and these most likely correspond to Mn₃As₂(I), Mn₃As₂(III), and Mn₄As₃. We do not have the experimental equipment to confirm the previously reported phase transitions at 750 and 775°C. The compounds Mn₃As₂(II) and Mn₅As₄

are formed only after prolonged annealing and apparently do not have their correspondence in the published phase diagrams.

STRUCTURE DETERMINATION

Crystals of Mn₄As₃, investigated on a Weissenberg camera, showed a C-centered monoclinic cell. The cell constants (Table 1) were obtained by a least-squares fit of Guinier powder data (Table 2) using α -quartz (*a* = 491.30

TABLE 2
Guinier Powder Pattern of Mn₄As₃^a

<i>h</i>	<i>k</i>	<i>l</i>	<i>Q</i> _o	<i>Q</i> _c	<i>I</i> _o	<i>I</i> _c
1	1	0	790	791	vw	4
1	1	1	937	937	w	13
0	0	3	1015	1015	m	21
4	0	-2	1111	1112	m	24
1	1	-2	1175	1175	w	18
3	1	0	1257	1256	vw	12
3	1	-1	1268	1268	s	38
1	1	2	1309	1309	s	71
3	1	1	1469	1469	vw	8
3	1	-2	1505	1506	w	14
4	0	-3	1541	1541	w	12
1	1	-3	1705	1705	vw	9
0	0	4	1803	1804	w	12
3	1	2	1908	1908	vs	86
3	1	-3	1968	1968	w	15
5	1	-1	2132	2131	s	43
6	0	-2	2139	2140	s	51
5	1	0	2187	2186	s	36
2	0	4	2304	2304	s	44
5	1	1	2466	2466	w	19
3	1	3	2575	2573	vw	7
3	1	-4	2658	2657	vs	100
0	2	0	2932	2932	vs	63
5	1	2	2972	2972	vw	15
4	0	4	3268	3270	vw	8
2	0	5	3387	3386	vw	6

^a The diagram was recorded with CuK α ₁ radiation. All observed reflections and all reflections with calculated intensities *I*_c > 5 are given. The *Q* values are defined by *Q* = 100/*d*² (nm⁻²). The observed intensities *I*_o are abbreviated as follows: vw—very very weak, m—medium, vs—very very strong.

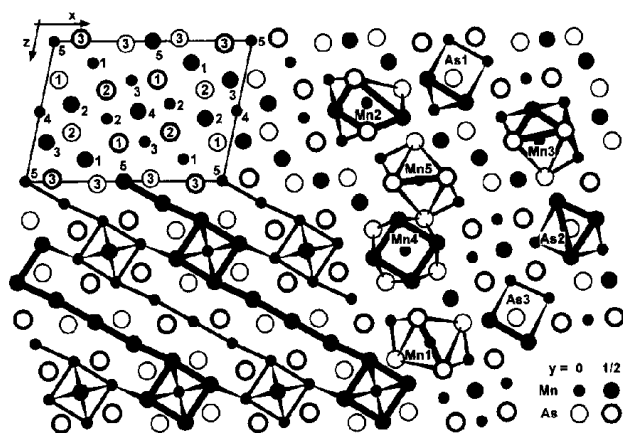


FIG. 1. Crystal structure and coordination polyhedra of Mn_4As_3 . In the lower left-side corner the Mn—Mn bonds are indicated. Single-digit numbers correspond to the atom designations.

pm and $c = 540.46$ pm) as a standard. Intensity data were collected from a single crystal with the dimensions $0.13 \times 0.02 \times 0.03$ mm³ on an automated four-circle diffractometer (Enraf Nonius CAD4) using graphite-monochromated $\text{MoK}\alpha$ radiation, a scintillation counter, and a pulse-height discriminator. The background was measured on both sides of each $\theta/2\theta$ scan. The intensities of 5023 reflections were recorded within the whole reciprocal space up to $2\theta = 90^\circ$. An empirical absorption correction was applied using psi scan data. The ratio of the highest to the lowest transmission was 1.22. Equivalent reflections were averaged ($R_i = 0.026$) and weak reflections ($<3\sigma$) were omitted.

The structure was determined by Patterson and successive Fourier syntheses and refined by full-matrix least-squares cycles using atomic scattering factors (20), corrected for anomalous dispersion (21). A parameter accounting for secondary isotropic extinction was optimized and the weighting scheme reflected the counting statistics. Refining the occupancy and the thermal parameters together revealed no deviations from the ideal occupancies greater than 0.5%. Therefore, the ideal occupancies were assumed during the final cycles. A conventional residual of $R = 0.027$ resulted for 1394 structure factors and 62 variable parameters. The final difference Fourier synthesis showed electron densities of $+1.0 e^-/\text{\AA}^3$ as the highest and $-1.2 e^-/\text{\AA}^3$ as the lowest values. The final positional parameters and the interatomic distances are listed in Tables 3 and 4. The anisotropic thermal parameters and the structure factors are available from the authors.

DISCUSSION

The structure of Mn_4As_3 (Fig. 1) is isotypic with that of the high-temperature modification of V_4As_3 (23). It con-

TABLE 3
Atomic Parameters of Mn_4As_3^a

Atom	$C2/m$	x	y	z	B
Mn1	4i	0.22021(5)	0	0.15675(7)	1.100(9)
Mn2	4i	0.34804(5)	0	0.55192(6)	0.840(8)
Mn3	4i	0.43466(5)	0	0.28198(7)	0.823(8)
Mn4	2c	0	0	$\frac{1}{2}$	0.74(1)
Mn5	2a	0	0	0	0.96(1)
As1	4i	0.06488(3)	0	0.27541(4)	0.704(5)
As2	4i	0.18384(3)	0	0.64986(4)	0.682(5)
As3	4i	0.36706(3)	0	0.01855(4)	0.874(6)

^a The atomic parameters were standardized by the program STRUCTURE TIDY (22). The last column contains the equivalent isotropic B values ($\times 10^{-4}$, in units of pm²) of the ellipsoidal displacement parameters.

tains a variety of coordination polyhedra for both atomic species as were also observed for the other manganese arsenides with similar composition. The average interatomic distances roughly reflect the different coordination numbers (CN). They decrease from 264.7 and 260.4 pm for Mn1 and Mn5 with octahedral arsenic coordination over 261.2 and 256.6 pm for Mn2 and Mn3, both with square-pyramidal coordination, to 254.0 pm for Mn4 with quadratic arsenic environment. In addition to these strongly bonded arsenic neighbors the manganese atoms have between two (Mn1 and Mn5) and eight (Mn4) manganese neighbors at distances covering the range from 279.7 to 319.9 pm. All of these Mn—Mn interactions may be

TABLE 4
Interatomic Distances of Mn_4As_3^a

Mn1:	1As1	257.5	Mn4:	2As1	249.3
	1As3	259.5		2As2	258.6
	2As3	261.0		4Mn3	279.7
	2As2	274.6		4Mn2	287.0
	1Mn3	287.9		Mn5:	4As3
1Mn5	302.5	2As1	261.4		
Mn2:	1As2	256.9	As1:	2Mn1	302.5
	2As1	259.5		1Mn4	249.3
	2As2	265.0		2Mn3	255.1
	2Mn4	287.0		1Mn1	257.5
	1Mn3	301.9		2Mn2	259.5
Mn3:	1Mn3	305.9	As2:	1Mn5	261.4
	2Mn2	319.9		1Mn2	256.9
	1As3	251.0		1Mn4	258.6
	2As1	255.1		2Mn3	260.8
	2As2	260.8		2Mn2	265.0
	2Mn4	279.7		2Mn1	274.6
	1Mn1	287.9		As3:	1Mn3
1Mn2	301.9	1Mn1	259.5		
1Mn2	305.9	2Mn5	259.9		
			2Mn1	261.0	

^a All distances shorter than 354 pm are listed. Standard deviations are all equal to or smaller than 0.1 pm.

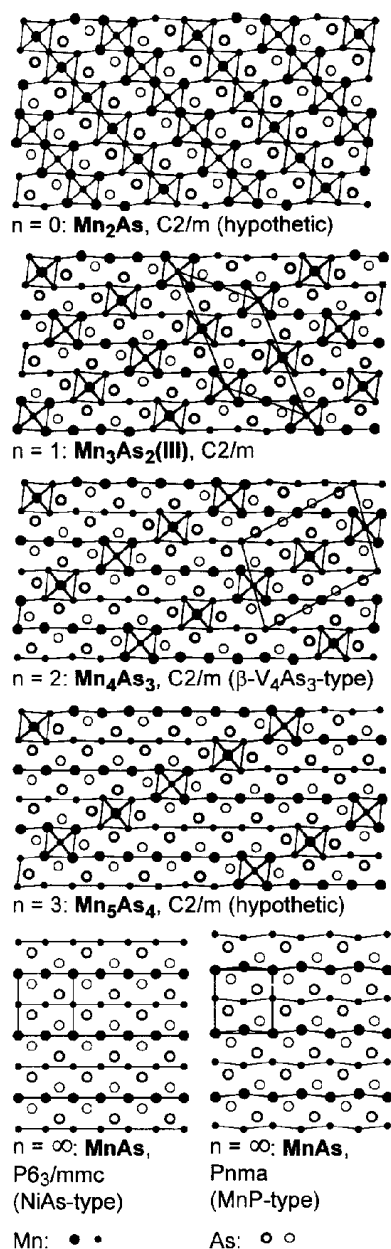


FIG. 2. Crystal structures of a series of manganese arsenides with the general composition $\text{Mn}_{2+n}\text{As}_{1+n}$. Of these the compounds $\text{Mn}_3\text{As}_2(\text{III})$, Mn_4As_3 , and the two modifications of MnAs are known and their unit cells are indicated. The others are hypothetical compounds. All atoms are located at two heights of the projection direction. All Mn—Mn bonds shorter than 320 pm are indicated.

considered as weakly bonding. Nevertheless, the thermal parameters of the manganese atoms reflect mainly the arsenic coordination. They are large for the Mn1 and Mn5 atoms (Table 3) with octahedral arsenic environment, smaller for the Mn2 and Mn3 atoms with square-pyramidal arsenic coordination, and the smallest for the Mn4 atom with quadrangular arsenic coordination. The three different

arsenic atoms have bicapped trigonal prismatic coordination (As2, average As—Mn distance 264.5 pm), monocapped trigonal prismatic coordination (As1, average As—Mn distance 256.8 pm), and noncapped trigonal prismatic coordination (As3, average As—Mn distance 258.7 pm).

In Figs. 2 and 3 we show projections of the various manganese arsenide structures along a short translation period emphasizing the metal—metal bonding. In all of these structures the atoms are situated at only two levels of the projection direction. It can be seen (Fig. 2) that the structure of Mn_4As_3 is a member (with $n = 2$) of a series of closely related structures with the general composition $\text{Mn}_{2+n}\text{As}_{1+n}$. Another representative (with $n = 1$) is the structure of $\text{Mn}_3\text{As}_2(\text{III})$ (16). The two modifications of MnAs (10–12) are end members of this series with $n = \infty$. The structure of Mn_2As (with $n = 0$) and Mn_5As_4 (with $n = 3$) have not been realized up to now, and this seems to be the case also for the other members of this series with $n > 3$. For the system vanadium—arsenic the corresponding series $\text{V}_{2+n}\text{As}_{1+n}$ has been recognized (24), although so far only the compounds β - V_4As_3 ($n = 2$) and VAs ($n = \infty$) are known for that system. Nevertheless, a structure for the hypothetical compound V_3As_2 has been proposed (24) which in fact is realized by $\text{Mn}_3\text{As}_2(\text{III})$.

Octahedral Mn_6 clusters occur in most compounds shown in Fig. 2. They form strings by sharing corners

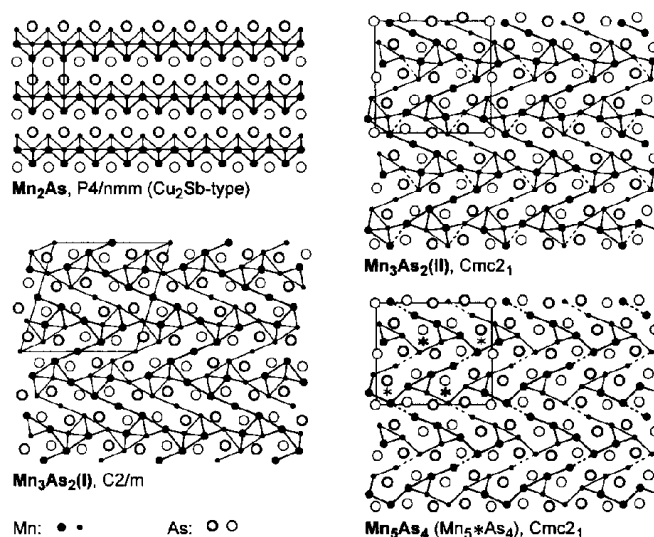


FIG. 3. Crystal structures of the manganese arsenides Mn_2As , $\text{Mn}_3\text{As}_2(\text{I})$, $\text{Mn}_3\text{As}_2(\text{II})$, and Mn_5As_4 . Atoms drawn with light and heavy symbols are separated from each other by half a translation period of the projection direction. All Mn—Mn bonds shorter than 322 pm are indicated; in addition Mn—Mn bonds of 326.7 pm in $\text{Mn}_3\text{As}_2(\text{II})$ and 328.1 pm in Mn_5As_4 are drawn with dashed lines, while the Mn—Mn bonds of 322.3 pm in $\text{Mn}_3\text{As}_2(\text{II})$ are omitted to emphasize the similarities of the structures. The structure of Mn_5As_4 is closely related to that of $\text{Mn}_3\text{As}_2(\text{II})$ (Mn_6As_4) from which it can be derived by the formation of vacancies which are indicated by asterisks.

along the projection direction. Perpendicular to that direction these octahedra are linked via metal-metal bonded chains. These chains increase in length with increasing value of n . For the two end-members of this series with the composition MnAs and $n = \infty$ the octahedra have disappeared. In the NiAs -type modification of MnAs the metal-metal bonded chains are parallel to the hexagonal axis.

The close relationships of the intergrowth structures $\text{Mn}_3\text{As}_2(\text{II})$ and Mn_5As_4 have been discussed before (14). Both structures contain building elements of the hexagonal NiAs and the "filled" NiAs structure of Ni_2In . This is also the case for $\text{Mn}_3\text{As}_2(\text{I})$ (15). In Fig. 3 these structures are represented in a way which allows us to recognize their similarity with the structure of Mn_4As_3 and the other structures of Fig. 2. It can be seen that the Cu_2Sb -type structure of Mn_2As shown in Fig. 3 is closely related to the hypothetical manganese arsenide Mn_2As of Fig. 2.

ACKNOWLEDGMENTS

We thank Dipl.-Ing. U. Rodewald and Dr. M. H. Möller for the collection of the single-crystal diffractometer data and Mr. K. Wagner for the work on the scanning electron microscope. We also acknowledge Dr. G. Höfer (Heraeus Quarzschmelze) for a generous gift of silica tubes. This work was supported by the Deutsche Forschungsgemeinschaft and the Fonds der Chemischen Industrie.

REFERENCES

1. W. Jeitschko and P. C. Donohue, *Acta Crystallogr. Sect. B* **31**, 574 (1975).
2. D. J. Braun and W. Jeitschko, *Z. Anorg. Allg. Chem.* **445**, 157 (1978).
3. W. Jeitschko, R. Rühl, U. Krieger, and C. Heiden, *Mater. Res. Bull.* **15**, 1755 (1980).
4. B. I. Nöling and L.-E. Terenius, *Acta Chem. Scand. Ser. A*, **34**, 311 (1980).
5. R. Rühl and W. Jeitschko, *Acta Crystallogr. Sect. B* **37**, 39 (1981).
6. H. Nowotny, R. Funk, and J. Pesl, *Monatsh. Chem.* **82**, 513 (1951).
7. H. Nowotny and F. Halla, *Z. Phys. Chem. Abt. B* **36**, 322 (1937).
8. A. E. Austin, E. Abelson, and W. H. Cloud, *J. Appl. Phys. Suppl.* **33**, 1356 (1962).
9. W. Jeitschko and V. Johnson, *Acta Crystallogr. Sect. B* **28**, 1971 (1972).
10. R. H. Wilson and J. S. Kasper, *Acta Crystallogr.* **17**, 95 (1964).
11. J. B. Goodenough and J. A. Kafalas, *Phys. Rev.* **157**, 389 (1967).
12. A. Zieba, K. Selte, A. Kjekshus, and A. F. Andresen, *Acta Chem. Scand. Ser. A* **32**, 173 (1978).
13. H. Okamoto, *Bull. Alloy Phase Diagrams* **10**, 549 and 607 (1989).
14. M. H. Möller and W. Jeitschko, *Z. Kristallogr.* **204**, 77 (1993).
15. L. H. Dietrich, W. Jeitschko, and M. H. Möller, *Z. Kristallogr.* **190**, 259 (1990).
16. M. F. Hagedorn and W. Jeitschko, *J. Solid State Chem.* **113**, 257 (1994).
17. J. B. Brauer, *U.S. Dep. Commer., Off. Tech. Serv., PB Rep.* **153, 264**, 54 pp. (1960); *Chem. Abs.* **58**, 6527 (1963).
18. M. F. Hagedorn and W. Jeitschko, *Z. Kristallogr. Suppl.* **5**, 93 (1992).
19. M. Yuzuri and M. Yamada, *J. Phys. Soc. Jpn.* **15**, 1845 (1960).
20. D. T. Cromer and J. B. Mann, *Acta Crystallogr. Sect. A*, **24**, 321 (1968).
21. D. T. Cromer and D. Liberman, *J. Chem. Phys.* **53**, 1891 (1970).
22. L. M. Gelato and E. Parthé, *J. Appl. Crystallogr.* **20**, 139 (1987).
23. R. Berger, *Acta Chem. Scand. Ser. A* **28**, 771 (1974).
24. S. Andersson, H. Annehed, L. Stenberg, and R. Berger, *J. Solid State Chem.* **19**, 169 (1976).